

Spectropolarimetry of the Type Ia Supernova 2012fr^{*}

J.R. Maund^{1,2,3†}, J. Spyromilio⁴, P.A. Höflich⁵, J.C. Wheeler⁶, D. Baade⁴,
A. Clocchiatti⁷, F. Patat⁴, E. Reilly¹, L. Wang⁸ & P. Zelaya⁷

¹ *Astrophysics Research Centre, School of Mathematics and Physics, Queen’s University Belfast, Belfast, BT7 1NN, Northern Ireland, U.K.*

² *Dark Cosmology Centre, Niels Bohr Institute, University of Copenhagen, Juliane Maries Vej 30, 2100 Copenhagen, DK.*

³ *Royal Society Research Fellow*

⁴ *ESO - European Organisation for Astronomical Research in the Southern Hemisphere, Karl-Schwarzschild-Str. 2, 85748 Garching b. München, Germany*

⁵ *Department of Physics, Florida State University, Tallahassee, Florida 32306-4350, U.S.A.*

⁶ *Department of Astronomy and McDonald Observatory, The University of Texas, 1 University Station C1402, Austin, Texas 78712-0259, U.S.A.*

⁷ *Departamento de Astronomía y Astrofísica, Pontificia Universidad Católica Casilla 306, Santiago 22, Chile*

⁸ *Department of Physics, Texas A&M University, College Station, Texas 77843-4242, U.S.A.*

9 October 2018

ABSTRACT

Spectropolarimetry provides the means to probe the 3D geometries of Supernovae at early times. We report spectropolarimetric observations of the Type Ia Supernova 2012fr at four epochs: -11, -5, +2 and +24 days, with respect to B -lightcurve maximum. SN 2012fr is a normal Type Ia SN, similar to SNe 1990N, 2000cx and 2005hj (that all exhibit low velocity decline rates for the principal Si II line). The SN displays high velocity components at -11 days that are highly polarized. The polarization of these features decreases as they become weaker from -5 days. At +2 days, the polarization angles of the low velocity components of silicon and calcium are identical and oriented at 90° relative to the high velocity Ca component. In addition to having very different velocities, the high and low velocity Ca components have orthogonal distributions in the plane of the sky. The continuum polarization for the SN at all four epochs is low $< 0.1\%$. We conclude that the low level of continuum polarization is inconsistent with the merger-induced explosion scenario. The simple axial symmetry evident from the polarization angles of the high velocity and low velocity Ca components, along with the presence of high velocity components of Si and Ca, is perhaps more consistent with the pulsating delayed detonation model. We predict that, during the nebular phase, SN 2012fr will display blue-shifted emission lines of Fe-group elements.

Key words: supernovae:general – supernovae:individual:2012fr

1 INTRODUCTION

Type Ia Supernovae (SNe) are energetic events resulting from the thermonuclear explosions of carbon-oxygen Chandrasekhar mass white dwarfs (WDs), in either single or double degenerate progenitor systems (Branch et al. 1995). The exact nature of the explosion mechanism behind Type Ia SNe is unknown, but a number of theoretical models have been proposed: deflagrations (Gamezo et al. 2004; Röpke et al. 2006), detonations (Arnett 1969), delayed detonations (Khokhlov 1991a), pulsating delayed detonations (Khokhlov 1991b; Khokhlov et al. 1993) or the mergers of two WDs (Webbink 1984; Pakmor et al. 2012). A key differentiating factor between these different models, with different physical considerations, is the geometry of the resulting explosion. Spectropolarimetry permits the direct observation of the 3D geometries of SN

explosions and provides, therefore, a direct probe of the underlying physics behind these explosions (for a review, see Wang & Wheeler 2008).

In general, Type Ia SNe are characterized by low levels of polarization, that decrease as time and the depth into the ejecta increase. Previous studies have shown that photometric and spectroscopic properties of Type Ia SNe are intimately tied to the geometry of these events, through the correlation of the polarization (specifically of the Si II $\lambda 6355$ feature p_{SiII}) with the lightcurve decline parameter $\Delta m_{15}(B)$ (Wang et al. 2007) and the decline rate of the velocity at the absorption minimum \dot{v}_{SiII} (Maund et al. 2010).

Here we report early spectropolarimetric observations of the Type Ia SN 2012fr. SN 2012fr was discovered by Klotz et al. (2012) on 2012 Oct 27.05 (UT) in the galaxy NGC 1365 ($3''$ East and $52''$ North of the nucleus). Based on previous observations of NGC 1365, the SN was discovered $< 3d$ post-explosion (Klotz et al. 2012). Childress et al. (2012) and Buil (2012) spectroscopically classified SN 2012fr as being a normal Type Ia SN. The

^{*} Based on observations made with ESO Telescopes at the Paranal Observatory, under program 290.D-5009 and 290.D-5006.

[†] Email: j.maund@qub.ac.uk

Table 1. Log of Spectropolarimetric Observations

Object	Date (UT)	Exposure (s)	Mean Airmass	Epoch* (days)
SN 2012fr	2012 Nov 1.07	4×170	1.56	-11
LTT1020 [‡]	2012 Nov 7.06	30	1.20	
SN 2012fr	2012 Nov 7.24	4×100	1.03	-5
LTT1020 ^{†‡}	2012 Nov 14.19	4×30	1.09	
LTT1020 [‡]	2012 Nov 14.19	8×30	1.08	
SN 2012fr	2012 Nov 14.22	4×100	1.03	+2
SN 2012fr	2012 Nov 14.23	4×80	1.04	+2
SN 2012fr [†]	2012 Nov 14.23	4×30	1.04	+2
SN 2012fr	2012 Dec 06.31	16×125	2.02	
G94-48 [‡]	2012 Dec 07.01	4×60	1.49	+24

* Relative to the maximum of the *B*-band lightcurve on 2012 Nov 12.04

† Observations conducted with the quarter wavelength retarder plate.

‡ Flux standard.

heliocentric recessional velocity for NGC 1365¹ is 1636 km s^{-1} . Contreras et al. (2013, in prep.) report that the *B*-band light curve maximum occurred at 2012 Nov 12.04 and measured $\Delta m_{15}(B) = 0.80$.

2 OBSERVATIONS AND DATA REDUCTION

Spectropolarimetric observations of SN 2012fr were conducted using the European Southern Observatory (ESO) Very Large Telescope (VLT) Antu Unit Telescope and the Focal Reducer and low dispersion Spectrograph (FORs; Appenzeller et al. 1998). The observations were made at four separate epochs, and a log of the observations is presented in Table 1. The data were acquired using the 300V grism and GG435 order separation filter (to prevent second order contamination in the red portion of the spectrum), providing a wavelength range of $4500 - 9300 \text{ \AA}$ with resolution $\sim 11.8 \text{ \AA}$ at 6000 \AA . At the +2d, observations were conducted with both the half-wavelength and quarter wavelength retarder plates, to measure the linear (*Q* and *U*) and circular (*V*) Stokes parameters, respectively. The data were reduced using IRAF² following the method presented by Maund et al. (2007). The reduction procedure was identical for observations conducted with half- and quarter-wavelength retarder plates. Flux spectra of the target SN were calibrated using observations of a flux standard acquired with the polarimetry optics in place. The Stokes parameters were rebinned to 15 \AA , slightly larger than one resolution element, to increase the level of signal to noise.

¹ Quoted from the NASA/IPAC Extragalactic Database - <http://ned.ipac.caltech.edu>

² IRAF is distributed by the National Optical Astronomy Observatory, which is operated by the Association of Universities for Research in Astronomy (AURA) under cooperative agreement with the National Science Foundation.

3 RESULTS

The polarization and flux spectra for SN 2012fr at the four observational epochs are presented in Figure 1. We compared the flux spectra at each epoch with those of other Type Ia SNe using *GELATO*³ (Harutyunyan et al. 2008). The first two flux spectra appear similar to SN 1990N at -13 and -7d (relative to *B*-band maximum; Leibundgut et al. 1991) and to the “Branch normal” SN 2005hj (Quimby et al. 2007); whilst the later spectra appear similar to 2000cx (Li et al. 2001).

At the first epoch, the Si II $\lambda 6355$ line is composed of two separate absorption components, a high velocity (HV) component at $-20\,000 \text{ km s}^{-1}$ and a low velocity (LV) component at $-12\,800 \text{ km s}^{-1}$. In the later epochs, Si II is dominated by the narrow LV component, although HV absorption is discernible at the second epoch. Based on the measured decline of the velocity of the Si II LV component over the four epochs ($\dot{v}_{SiII} = 25 \pm 7 \text{ km s}^{-1} \text{ d}^{-1}$), SN 2012fr is a member of the Low Velocity Gradient (LVG) group of Type Ia SNe (Benetti et al. 2005). The HV component of Si II appears detached from the LV component, and we find the velocity at the blue edge of the absorption trough at -11d is the same as the velocity measured at absorption minimum for the Ca II Infrared Triplet (IR3), as observed by Quimby et al. (2007) in spectra of SN 2005hj.

At the first two epochs, the Ca II IR3 profile (shown in Figure 2) displays a significant HV component ($-28\,600$ and $-23\,500 \text{ km s}^{-1}$, for the first and second epochs respectively), with three weaker LV components (labeled A, B and C in Fig. 2). The HV component appears in the last two epochs, but as a much weaker absorption, while the strongest absorption arises from the “A” LV component. At +2d, we measure velocities of the three LV components to be $-10\,900$, $-8\,200$ and $-8\,000 \text{ km s}^{-1}$, relative to Ca II $\lambda\lambda 8498, 8542, 8662$, respectively. The “saw tooth” pattern of absorption components (+2d) is similar to that observed for SN 2000cx at +7d post-maximum (Li et al. 2001). We suggest that the LV components arise from the partially resolved individual lines of which the IR3 is composed.

At each epoch the polarization spectrum is characterized by a relatively low level of polarization $0.3 - 0.4\%$. Although peaks in the polarization spectra may be associated with the blue Fe lines and the S II absorption features ($5200 - 5400 \text{ \AA}$), the most significantly polarized features are the Si II and Ca II IR3 lines. At the first two epochs, the apparent rise in polarization at longer wavelengths coincides with the increasing uncertainty on the polarization commensurate with the decreasing signal-to-noise. The apparent polarization at $\sim 7600 \text{ \AA}$ is due to the significant telluric absorption around that wavelength and is not intrinsic to the SN. On the Stokes *Q* – *U* plane (see Figure 3), the data at all epochs are characterized by a central concentration of points, with significant departures at wavelengths associated with Si II and Ca II features.

Stokes *V* was measured at +2d to be $0 \pm 0.2\%$, consistent with there being no circular polarization over the entire wavelength range; as was the case with the previous reported broad-band polarimetric measurement of the Type I SN 1972E (Wolstencroft & Kemp 1972) and spectropolarimetry of Type Ia SN 1983J (McCall et al. 1984). The equipment used for the observations made of SN 1972E, one month after maximum light, is not identified. SN 1983J was observed around maximum light with a 4-m telescope and no solid-state detector. Our VLT CCD data for SN 2012fr, at maximum light, should set the tightest limits to date on circular polarization

³ <http://gelato.tng.iac.es/>

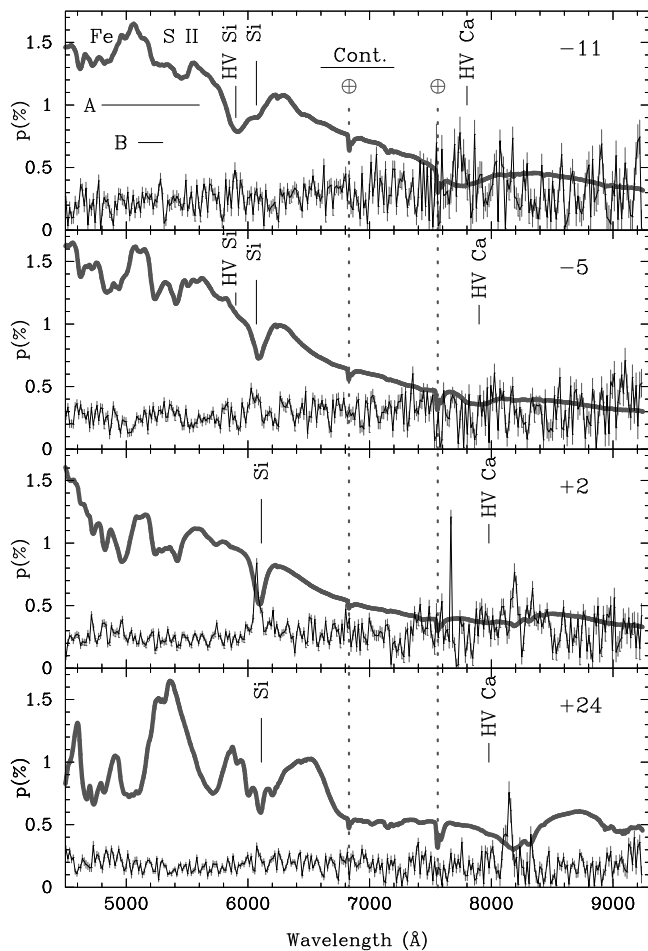


Figure 1. Polarization spectra of SN 2012fr at -11, -5, +2 and +24d relative to *B*-lightcurve maximum. A scaled flux spectrum ($\text{erg s}^{-1} \text{cm}^{-2} \text{s}^{-1}$) is shown as the thick line. All spectra have been corrected for the recessional velocity of the host galaxy. The polarization spectra have not been corrected for the interstellar polarization component. The wavelength ranges used for the two estimates of the interstellar polarization (labelled “A” and “B”) and for measuring the continuum polarization (labelled “Cont.”) are indicated by the horizontal bars. The principal telluric lines are indicated by the \oplus symbol.

of any Type Ia SN (or even yield a marginal detection). We will pursue this in a separate study.

4 ANALYSIS

The correct interpretation of the intrinsic polarization of SNe requires the removal of the interstellar polarization (ISP). We estimated the degree of the ISP directly from the observations, under the assumption that regions of the SN spectra are intrinsically unpolarized due to line blanketing of Fe lines (Howell et al. 2001; Chornock et al. 2006; Maund et al. 2010; Patat et al. 2009). We identify two regions in the spectrum of SN 2012fr that are likely to be intrinsically depolarized due to multiple overlapping Fe lines at the first three epochs: regions A (4800 – 5600Å) and B (5100 – 5300Å), as shown in Fig. 1. At +24d it is apparent that lines in these regions have ceased to be blended and we see strong individual line profiles, so it was not included in the determination of the ISP. The weighted average Stokes parameters

over these wavelength ranges were used as a measure of the ISP: $\langle Q_{ISP}^A \rangle = 0.24 \pm 0.04\%$, $\langle U_{ISP}^A \rangle = 0.00 \pm 0.04\%$ and $\langle Q_{ISP}^B \rangle = 0.24 \pm 0.04\%$, $\langle U_{ISP}^B \rangle = 0.00 \pm 0.04\%$. These correspond to $p_{ISP} = 0.24 \pm 0.01\%$ and $\chi_{ISP} = 0.0 \pm 4.9^\circ$, roughly aligned with the position angle of SN 2012fr with respect to the nucleus of NGC 1365.

Under the assumption that the wavelength region 6600 – 7200Å is representative of the continuum (Patat et al. 2009), we the weighted average continuum polarization (after correction for the ISP) to be: $0.06 \pm 0.12\%$, $0.05 \pm 0.09\%$, $0.03 \pm 0.09\%$ and $0.06 \pm 0.07\%$ at -11, -5, +2 and +24d respectively, consistent with null polarization. The low level of continuum polarization is consistent with a spherical photosphere (with axial ratio > 0.95 ; Höflich 1991). After correction for the ISP, the only lines remaining with significant polarization are the Si II $\lambda 6355$ and Ca II IR3 lines.

At -11d, the polarization signal associated with Si II is dominated by the HV component at $0.40 \pm 0.06\%$, but as the optical depth of this component decreases we no longer observe it to be polarized by -5d; whilst the polarization signal of the LV component increases. On the Stokes $Q - U$ plane (see Figure 3), the polarization signals of the HV component (observed at -11d) and the LV component (at -5d) are found to be separated by $\Delta\chi \approx 20^\circ$ (which is evidence that the HV and LV components are physically separated, both in radial velocity and on the sky). Although the degree of polarization of the LV component increases from $0.30 \pm 0.05\%$ (at -5d) to $0.65 \pm 0.04\%$ (at +2d), the polarization angle remains the same, implying that the LV Si II line forming region is a single continuous region covering the photosphere. At +24d, we measure a reduced level of polarization of $0.20 \pm 0.03\%$ associated with the now weaker Si II absorption, accompanied by a rotation of the polarization angle through $\approx 70^\circ$.

At the first epoch, the HV component of Ca II shows the largest polarization of $0.85 \pm 0.13\%$; by -5d the degree of polarization decreases to $0.31 \pm 0.08\%$ (see Figure 2). At +2d, the polarization signal associated with Ca II is dominated by the LV component with $0.54 \pm 0.07\%$ (specifically the absorption “A” in Fig. 2). From Fig. 2 it is clear that the Stokes parameters associated with the HV component at earlier epochs are inverted with respect to the Stokes parameters of the LV components observed late (i.e. the signs of Stokes Q and U parameters for the HV component are opposite to those of the LV component); this is also visible as a rotation of the polarization angle of the Ca II features on Fig. 3. This implies that the HV and LV components arise from line forming regions that are not only kinematically distinct, but also orthogonal to each other on the plane of the sky. At +2 and +24d, the polarization angles of the strong Ca II absorption (arising from the LV component) are aligned with the highly polarized Si II feature observed at +2d, suggesting a common line forming region; however, the velocities of the LV Ca II components are lower and decline faster than for Si II $\lambda 6355$. At +24d, the polarization signal at the wavelength of the HV component is dominated by the polarization of the underlying LV component.

5 DISCUSSION & CONCLUSIONS

We have presented early spectropolarimetric observations of the Type Ia SN 2012fr; finding the degree of polarization to be generally low, except for significant line polarization associated with Si II and Ca II. At early times we see evidence for kinematically distinct HV components, which weaken significantly by +2d. Si-

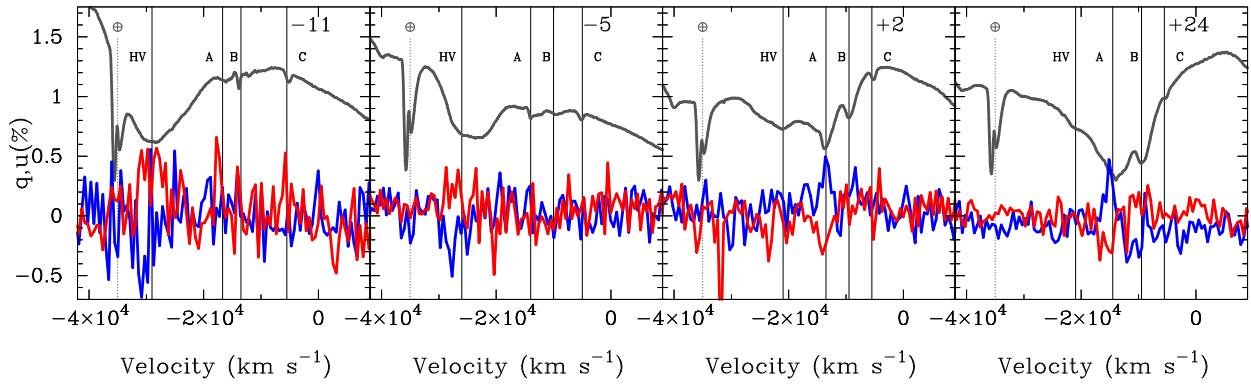


Figure 2. The Stokes Q (blue) and U (red) parameters across the Ca II IR3 at -11, -5, +2 and +24d, relative to B -lightcurve maximum. The Stokes parameters have been corrected for the ISP. The scaled flux spectrum is shown by the thick line. The velocity scale is defined relative to average wavelength of the Ca II IR3 (8579Å). The high velocity component is labeled “HV”, while the three LV components are labeled A-C. The principal telluric line is indicated by the \oplus symbol.

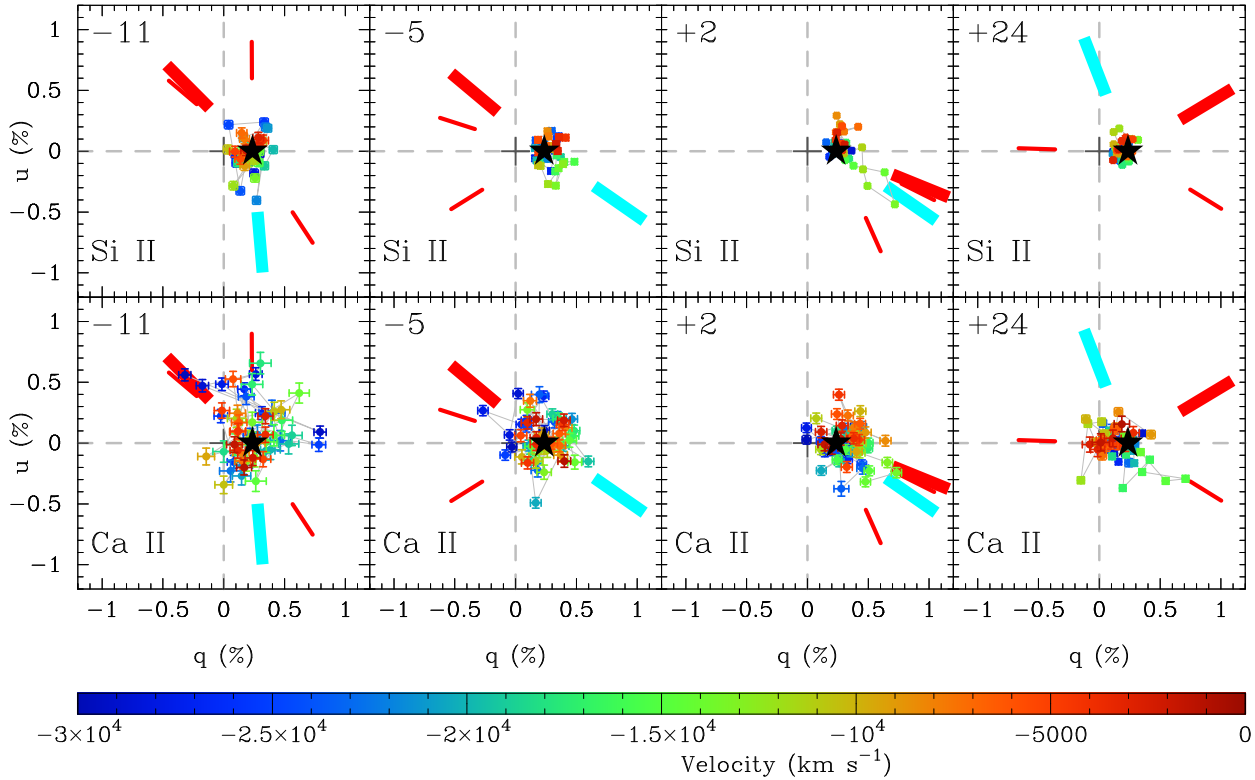


Figure 3. The polarization for the Si II $\lambda 6355$ (top row) and the Ca II IR3 (bottom row) lines on the Stokes $Q - U$ plane at -11, -5, +2 and +24d, relative to B -lightcurve maximum. The points are colour coded according to the velocity relative to the respective rest wavelengths for the two features. The data are not corrected for the ISP (the location of which is indicated by the \star). The thick radial lines indicate the polarization angles (on the Stokes $Q - U$ plane) for Si II (light blue) and the HV component of Ca II IR3 (red) (the LV components are indicated by narrow red radial lines).

multaneously, the strength of the LV components increases and their respective polarizations also increase, but at different polarization angles than the HV components. The low decline rate of the LV Si II velocity and the degree of polarization measured for the line at -5d adheres closely to the relationship established by Maund et al. (2010) (see their Figure 1) between these two parameters; and closely matches the values measured for the 1991T-like SN 1997br (Li et al. 1999; Wang et al. 2007). The degree of Si II polarization and the measured $\Delta m_{15}(B)$ also follows the correlation found by Wang et al. (2007). In comparison with the Maund

et al. sample, SN 2012fr is the only SN with $\Delta m_{15}(B) < 1$ that also exhibits low p_{SiII} and belongs to the LVG group. Based on the previous correlation established between Si II polarization and the characteristics of the late-time nebular spectrum (Maund et al. 2010; Maeda et al. 2010), we predict that the profiles of lines of Fe-group elements in the nebular spectrum of SN 2012fr will exhibit a blue shift.

The presence of short lived HV Ca II IR3 components in the spectra of Type Ia SNe is not unusual. Gerardy et al. (2004) modeled this feature, in SN 2003du, as arising from a low mass

($\sim 0.02M_{\odot}$) shell of primordial material from the circumstellar medium. Both HV Si II and Ca II were observed in the spectra of SN 2005hj (Quimby et al. 2007). The presence of these two features in a similar velocity space demands the presence of a large mass of SN processed material at high velocities, leading Quimby et al. to suggest an explosive origin for the shell through pulsating delayed detonations (PDDs; Khokhlov 1991a; Khokhlov et al. 1993) or mergers. The 3D signatures of these mechanisms, however, will be very different. Approximate spherical symmetry is expected to be maintained in the PDD model (although this must be verified with multidimensional simulations), but large scale asymmetries are expected in mergers. The overall low level of continuum polarization observed for SN 2012fr, however, is inconsistent with the asymmetric nickel distributions predicted by Pakmor et al. (2012) for violent mergers. The apparent orthogonality of the line forming regions for the HV and LV Ca II components observed for SN 2012fr, on the plane of the sky, is evidence for a simple axial symmetry. We also note that the slow rise time of the light curve of SN 2012fr and the low decline rate of the Si II velocity are consistent with the predictions of the PDD model (Khokhlov et al. 1993; Höflich & Khokhlov 1996).

The spectroscopic and photometric similarities between the low $\dot{v}_{Si II}$, low $\Delta m_{15}(B)$ SNe, such as 1990N, 2000cx and 2005hj, with SN 2012fr, suggest that these events may be similar events observed at similar orientations (possibly consistent with the PDD model).

ACKNOWLEDGMENTS

We thank the ESO Director General for awarding discretionary time for the observations and the observers at Paranal for conducting such exquisite observations. We thank Carlos Contreras and Jeffery Silverman for early notification of the results of their photometric monitoring of SN 2012fr. The research of JRM is supported through a Royal Society University Research Fellowship. The work of JCW is supported in part by NSF Grant AST-1109801. AC & PZ acknowledge support from Iniciativa Científica Milenio (MINECON, Chile) through the Millennium Center for Supernova Science (P10-064-F) and Basal grant CATA PFB 06/09 from CONICYT, Chile.

References

- Appenzeller I., Fricke K., Furtig W., Gassler W., Hafner R., Harkl R., Hess H.-J., Hummel W., et al. 1998, *The Messenger*, 94, 1
- Arnett W. D., 1969, *Ap&SS*, 5, 180
- Benetti S., Cappellaro E., Mazzali P. A., Turatto M., Altavilla G., Bufano F., Elias-Rosa N., Kotak R., Pignata G., Salvo M., Stanishev V., 2005, *ApJ*, 623, 1011
- Branch D., Livio M., Yungelson L. R., Boffi F. R., Baron E., 1995, *PASP*, 107, 1019
- Buil C., 2012, *Central Bureau Electronic Telegrams*, 3277, 3
- Childress M., Zhou G., Tucker B., Bayliss D., Scalzo R., Yuan F., Schmidt B., 2012, *Central Bureau Electronic Telegrams*, 3277, 2
- Chornock R., Filippenko A. V., Branch D., Foley R. J., Jha S., Li W., 2006, *PASP*, 118, 722
- Gamezo V. N., Khokhlov A. M., Oran E. S., 2004, *Physical Review Letters*, 92, 211102
- Gerardy C. L., Höflich P., Fesen R. A., Marion G. H., Nomoto K., Quimby R., Schaefer B. E., Wang L., Wheeler J. C., 2004, *ApJ*, 607, 391
- Harutyunyan A. H., Pfahler P., Pastorello A., Taubenberger S., Turatto M., Cappellaro E., Benetti S., Elias-Rosa N., Navasardyan H., Valenti S., Stanishev V., Patat F., Riello M., Pignata G., Hillebrandt W., 2008, *A&A*, 488, 383
- Höflich P., Khokhlov A., 1996, *ApJ*, 457, 500
- Höflich P., 1991, *A&A*, 246, 481
- Howell D. A., Höflich P., Wang L., Wheeler J. C., 2001, *ApJ*, 556, 302
- Khokhlov A., Mueller E., Höflich P., 1993, *A&A*, 270, 223
- Khokhlov A. M., 1991a, *A&A*, 245, 114
- Khokhlov A. M., 1991b, *A&A*, 245, L25
- Klotz A., Normand J., Conseil E., Parker S., Fabrega J., Maury A., 2012, *Central Bureau Electronic Telegrams*, 3277, 1
- Leibundgut B., Kirshner R. P., Filippenko A. V., Shields J. C., Foltz C. B., Phillips M. M., Sonneborn G., 1991, *ApJL*, 371, L23
- Li W., Filippenko A. V., Gates E., Chornock R., Gal-Yam A., Ofek E. O., Leonard D. C., Modjaz M., Rich R. M., Riess A. G., Treffers R. R., 2001, *PASP*, 113, 1178
- Li W. D., Qiu Y. L., Qiao Q. Y., Zhu X. H., Hu J. Y., Richmond M. W., Filippenko A. V., Treffers R. R., Peng C. Y., Leonard D. C., 1999, *AJ*, 117, 2709
- Maeda K., Benetti S., Stritzinger M., Röpke F. K., Folatelli G., Sollerman J., Taubenberger S., Nomoto K., Leloudas G., Hamuy M., Tanaka M., Mazzali P. A., Elias-Rosa N., 2010, *Nature*, 466, 82
- Maund J., Wheeler J., Patat F., Baade D., Wang L., Höflich P., 2007, *MNRAS*, 381, 201
- Maund J. R., Höflich P., Patat F., Wheeler J. C., Zelaya P., Baade D., Wang L., Clocchiatti A., Quinn J., 2010, *ApJL*, 725, L167
- Maund J. R., Wheeler J. C., Wang L., Baade D., Clocchiatti A., Patat F., Höflich P., Quinn J., Zelaya P., 2010, *ApJ*, 722, 1162
- McCall M. L., Reid N., Bessell M. S., Wickramasinghe D., 1984, *MNRAS*, 210, 839
- Pakmor R., Kromer M., Taubenberger S., Sim S. A., Röpke F. K., Hillebrandt W., 2012, *ApJL*, 747, L10
- Patat F., Baade D., Höflich P., Maund J. R., Wang L., Wheeler J. C., 2009, *A&A*, 508, 229
- Quimby R., Höflich P., Wheeler J. C., 2007, *ApJ*, 666, 1083
- Röpke F. K., Gieseler M., Reinecke M., Travaglio C., Hillebrandt W., 2006, *A&A*, 453, 203
- Wang L., Baade D., Patat F., 2007, *Science*, 315, 212
- Wang L., Wheeler J. C., 2008, *ARAA*, 46, 433
- Webbink R. F., 1984, *ApJ*, 277, 355
- Wolstencroft R. D., Kemp J. C., 1972, *Nature*, 238, 452